(1)

AD-A234 406

IMENTATION PAGE

Form Approved
OMB No. 0704-0188

1a. REPORT SECURITY CLASSIFICATION: UNCLASSIFIED	1b. RESTRICTIVE MARKINGS
2a. SECURITY CLASSIFICATION AUTHORITY	3. DISTRIBUTION/AVAILABILITY OF REPORT: Approved for public release; Distribution Unlimited
2b. DECLASSIFICATION/DOWNGRADING SCHEDULE	
4. PERFORMING ORGANIZATION REPORT NUMBER(S): PL-TR-91-2058	5. MONITORING ORGANIZATION REPORT NUMBER(S)
6a. NAME OF PERFORMING ORGANIZATION: Phillips Lab, Geophysics Directorate; 6b. OFFICE SYMBOL (If applicable): PHS	7a. NAME OF MONITORING ORGANIZATION: DTIC
6c. ADDRESS (City, State, and ZIP Code): Hanscom AFB, MA 01731-5000	7b. ADDRESS (City, State, and ZIP Code)
8a. NAME OF FUNDING/SPONSORING ORGANIZATION; 8b. OFFICE SYMBOL (If applicable)	9. PROCUREMENT INSTRUMENT IDENTIFICATION NUMBER
8c. ADDRESS (City, State, and ZIP Code)	10. SOURCE OF FUNDING NUMBERS

PROGRAM ELEMENT NO	PROJECT NO	TASK NO	WORK UNIT ACCESSION NO
61102F	2311	G3	27

11. TITLE (Include Security Classification)

Structure and Oscillations in Quiescent Filaments from Observations in He I λ 10830Å

12. PERSONAL AUTHOR(S)

Yi Zhang,* Oddbjorn Engvold,* and Stephen L. Keil

13a. TYPE OF REPORT	13b. TIME COVERED	14. DATE OF REPORT (Year, Month, Day)	15. PAGE COUNT
Reprint	FROM _____ TO _____	1991 March 26	18

16. SUPPLEMENTARY NOTATION *Institute of Theoretical Astrophysics, University of Oslo, P.O.Box 1029, Blindern, N-0315 Oslo 3, Norway
Reprinted from Solar Physics 132:63-80, 1991

17. COSATI CODES			18. SUBJECT TERMS (Continue on reverse if necessary and identify by block number)
FIELD	GROUP	SUB-GROUP	
03	02		solar, corona, prominence, oscillations

19. ABSTRACT (Continue on reverse if necessary and identify by block number)

Observations of two quiescent filaments show oscillatory variations in Doppler shift and central intensity of the He I λ10830 Å line. The oscillatory periods range from about 5 to 15 min. with dominant periods of 5, 9, and 16 min. The 5-min period is also detected in the intensity variations, after correction for atmospheric effects. Doppler shifts precede intensity variations by about one period. The possibility that the oscillations are Alfven waves is discussed. The Doppler signals of the filament form fibril-like structures. The fibrils are all inclined at an angle of about 25° to the long axis of the filament. The magnetic field has a similar orientation relative to the major direction of the filament, and the measured Doppler signals are apparently produced by motions along magnetic flux tubes threading the filament. The measured lifetimes of the small-scale fibrils of quiescent disk filaments are very likely a combined effect of intensity and reshuffling of the structures.

20. DISTRIBUTION/AVAILABILITY OF ABSTRACT	21. ABSTRACT SECURITY CLASSIFICATION
☐ UNCLASSIFIED/UNLIMITED ☒ SAME AS RPT ☐ DTIC USERS	UNCLASSIFIED

22a. NAME OF RESPONSIBLE INDIVIDUAL	22b. TELEPHONE (Include Area Code)	22c. OFFICE SYMBOL
Claire Caufield	(617) 377-4555	PL/SULLP

DD Form 1473, JUN 86 — Previous editions are obsolete. SECURITY CLASSIFICATION OF THIS PAGE: UNCLASSIFIED

POC: PL/PHS/R. Altrock/DSN 867-7542

DISCLAIMER NOTICE

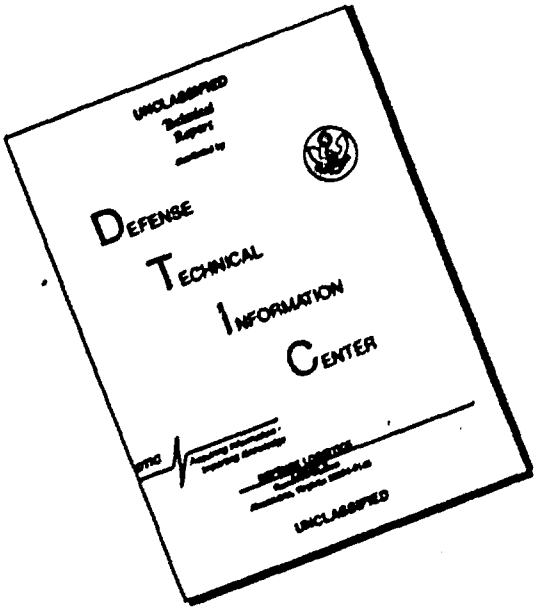

THIS DOCUMENT IS BEST QUALITY AVAILABLE. THE COPY FURNISHED TO DTIC CONTAINED A SIGNIFICANT NUMBER OF PAGES WHICH DO NOT REPRODUCE LEGIBLY.

STRUCTURE AND OSCILLATIONS IN QUIESCENT FILAMENTS FROM OBSERVATIONS IN He I λ10830 Å

YI ZHANG and ODDBJØRN ENGVOLD

Institute of Theoretical Astrophysics, University of Oslo, P.O. Box 1029 Blindern, N-0315 Oslo 3, Norway

and

STEPHEN L. KEIL

AFGL, Sacramento Peak, Sunspot, New Mexico 88349, U.S.A.

(Received 23 July, 1990; in revised form 23 October, 1990)

Abstract. Observations of two quiescent filaments show oscillatory variations in Doppler shift and central intensity of the He I λ10830 Å line.

The oscillatory periods range from about 5 to 15 min, with dominant periods of 5, 9, and 16 min. The 5-min period is also detected in the intensity variations, after correction for atmospheric effects. Doppler shifts precede intensity variations by about one period. The possibility that the oscillations are Alfven waves is discussed.

The Doppler signals of the filament form fibril-like structures. The fibrils are all inclined at an angle of about 25° to the long axis of the filament. The magnetic field has a similar orientation relative to the major direction of the filament, and the measured Doppler signals are apparently produced by motions along magnetic flux tubes threading the filament.

The measured lifetimes of the small-scale fibrils of quiescent disk filaments are very likely a combined effect of intensity modulations and reshuffling of the structures.

1. Introduction

The oscillatory character of velocities in quiescent prominences has been studied by several authors. Recent results are discussed by Tsubaki *et al.* (1988). Two types of oscillations have been found. The first type is a long-period oscillation. Malville and Schindler (1981) detected oscillations of a loop prominence of period 75 min. Similar oscillatory periods (50 to 64 min) have been observed in quiescent prominences by Wiehr, Stellmacher, and Balthasar (1984). Similarly, Suematsu *et al.* (1990) reported to have seen periods of about one hour in a large quiescent prominence. The second type has a much shorter period. Wiehr, Stellmacher, and Balthasar (1984) detected oscillations of periods from 3 to 8 min in Zeeman polarization of the Hα line. From analyses of CaII K line profiles Tsubaki and Takendi (1986) and Tsubaki, Ohnishi, and Suematsu (1987) measured periods in velocity variations of 160, 210, and 640 s. Short periods of 240 and 830 s have also been detected by Suematsu *et al.* (1990). All these studies were done in prominences observed at the solar limb. Oscillatory motions have not yet been detected in observations of prominences on the disk (filaments). Malherbe, Schmieder, and Mein (1981) and Malherbe *et al.* (1987) studied radial velocity both in Hα and CIV line in filaments, and concluded that oscillations could not be seen.

Ghenojian, Klepikov, and Stepanov (1990) concluded from polarimetric and spectro-

Solar Physics **132:** 63–80, 1991.

scopic observations of prominences that only the measured velocity variations in Doppler velocity are of solar origin. The periodic variations in such as line widths, intensity, and polarization are allegedly produced by some wave phenomena in our atmosphere.

The shorter periods could be local MHD waves, whereas the longer periods may represent eigenmodes of presumed loop-like structures themselves. The objective of the present study is to analyse the oscillatory nature of the vertical flow velocities in filaments using observations in the He I λ10830 A line.

The fine fibril structures of prominences are well visible in observations of subarcsecond seeing (Dunn, 1960; Engvold, 1976; Demoulin *et al.*, 1987). The lifetime of such structures is about 8 min or less, depending on size and brightness (Engvold, 1976, 1978). Generally, the fibrils are organized at some angle relative to the long axis of the filament (Simon *et al.*, 1986). From a sample of 70 prominences Tandberg-Hanssen and Anzer (1970) found that the field makes an angle $\alpha \simeq 15^\circ$ with the filament long axis. Other groups (Leroy, Bommier, and Sahal-Brechot, 1984; Kim, 1990) find angles of inclination about 25°. The shear of the magnetic field inferred from the data above is, conceivably, a necessary condition for the formation of prominences.

Assuming that the mass motions in filaments are channeled along the magnetic fibril structures one expects to see the magnetic topology reflected in the spatial pattern of the motions.

2. Observations and Data Processing

The observational data is part of 2-D spectral scans of a total of 17 different filaments observed during the period May 3 through 9, 1981, using the main spectrograph of the Vacuum Tower Telescope of the National Solar Observatory at Sacramento Peak (Dunn, 1969).

Each series of scans consists of 60 spectral frames (sometimes 90) recorded in rapid succession while the solar image drifted across the entrance slit of the spectrograph. The time difference between successive scans is 140 s. The slit positions of adjacent exposures are barely overlapping, and the data covers an area on the Sun of 76 × 100 arc sec^2. A 100 × 100 pixel CCD camera was used to record 100 arc sec by 6.0 A spectral sections centred on the chromospheric He I λ10830 A line. Each spectral exposure also contains the photospheric Si λ10827.109 A line, and the atmospheric water vapour line at λ10832.109 A. Both lines were used for calibration of the wavelength scale (cf. Breckinridge and Hall, 1973). Standard procedures were applied to correct the CCD images for variable pixel sensitivity and dark current.

The spectral dispersion corresponds to 3.86 mA per pixel, which is equivalent to 9.4 pixels per km s^{-1}. High-frequency noise was removed by appropriate smoothing of the data in both spatial and spectral directions. The position of the He I line was measured as the position of the central minimum intensity, and as the 'center of mass' of the deepest 25%$_0$ of the line. No significant differences in the results from the two methods were found. The latter definition has been used for the results presented here.

The He I line is very weak in the chromosphere, but quite strong in absorption in disk filaments, and consequently bright in emission in prominences observed at the limb (Giovanelli, Hall, and Harvey, 1972). The absence of a chromospheric absorption line makes the interpretations of the He I line absorption in filaments less complicated than in the cases of the Ca II H and K, and hydrogen Balmer lines.

3. Results

The filament of May 4 is displayed in the two images of Figure 1, which are reconstructed from one series of spectral frames. One image gives the contour map of the central intensity of He I λ10830 Å and the other shows the corresponding line-of-sight velocity. One notices that the velocity map resolves finer details and smaller structures than the intensity image.

3.1. Orientation of Fibril Structures in the Filament

The fine-scale velocity structures vary with time. Both the amplitudes of line shifts, as well as their positions, are changing. The velocity field appears in the form of fibril structures, which all are aligned systematically relative to the long axis of the filament (see Figure 1(b)). The angles of inclination range typically between 17° and 35°, with an average value of $\simeq 26°$ over the 27.5 min duration of the time series.

The mean half width of the filament fibril structures, i.e., the FWHM in the direction perpendicular to their long axes, are typically 1–3 arc sec. The true widths are most likely smaller, and the measured widths are very likely given by the spatial resolution in the data which is $\simeq 1$ arc sec.

The measured angles of inclination are similar to the earlier noted shear of the magnetic field (Leroy, 1988; Kim, 1990). This observation suggests that the observed velocity fibrils truly represent mass motion in magnetic flux tubes which are threading the filament.

3.2. Oscillations

3.2.1. *Velocity*

The time behaviour of the velocity signal is measured over 2.5×3.0 arc sec^2 areas at several positions along the filament fibrils. The results from the 27.5 min long time series of images of 4 May are shown in Figure 3. The similarity in the velocity signals along a given fibril means that the entire fibril structure is activated which would be the case if the fibrils are magnetic flux tubes. The power spectra for fixed points along the fibrils show peaks at frequencies corresponding to periods in the range from 9 to 14 min. The amplitudes of velocity variations are typically ± 0.5 km s^{-1}.

The filament of 3 May was observed for 97 min, and provides an opportunity to search for periods of oscillations over a larger range. Figures 4(a) and 4(b) show the

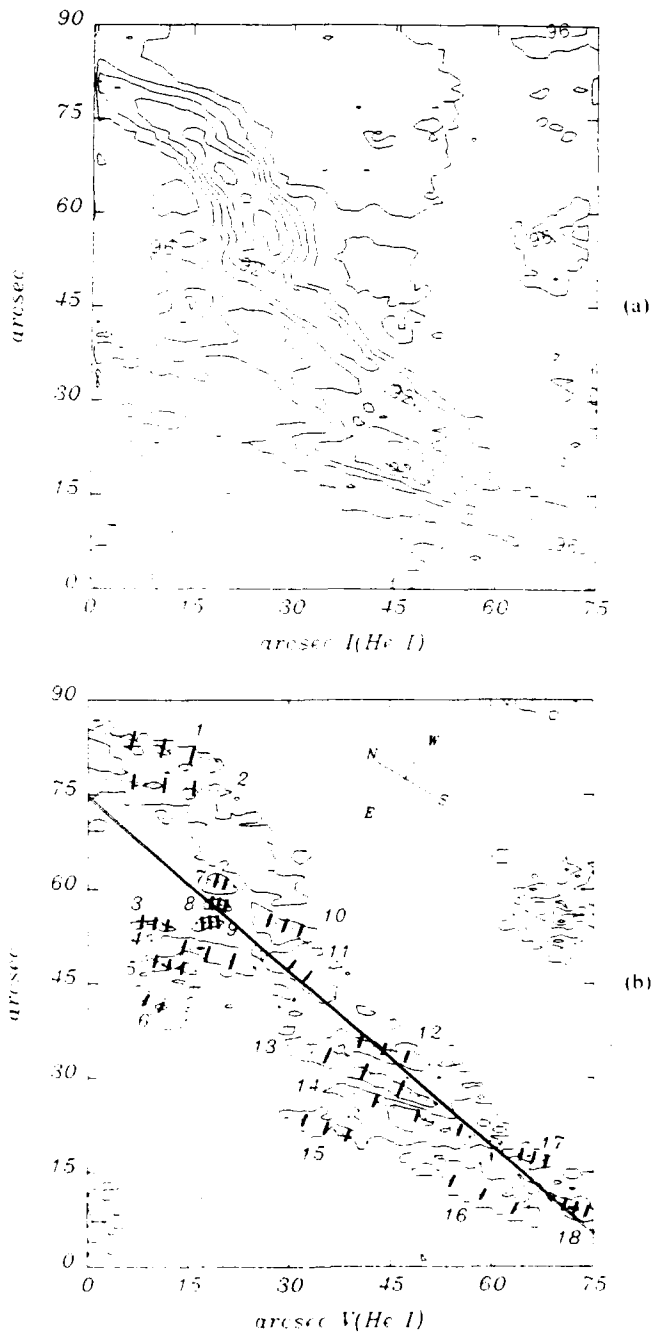

Fig. 1. (a) The central line intensity map of He I λ10830 Å in a quiescent filament observed on May 4, 1981, 13:41:00–13:42:20 UT. (b) The corresponding velocity map derived from the He I line. The long axis of the quiescent filament is indicated by the straight line and the axes of velocity fibrils are drawn with broken straight lines. The sampling window size is shown by the square box in the lower left of the frame.

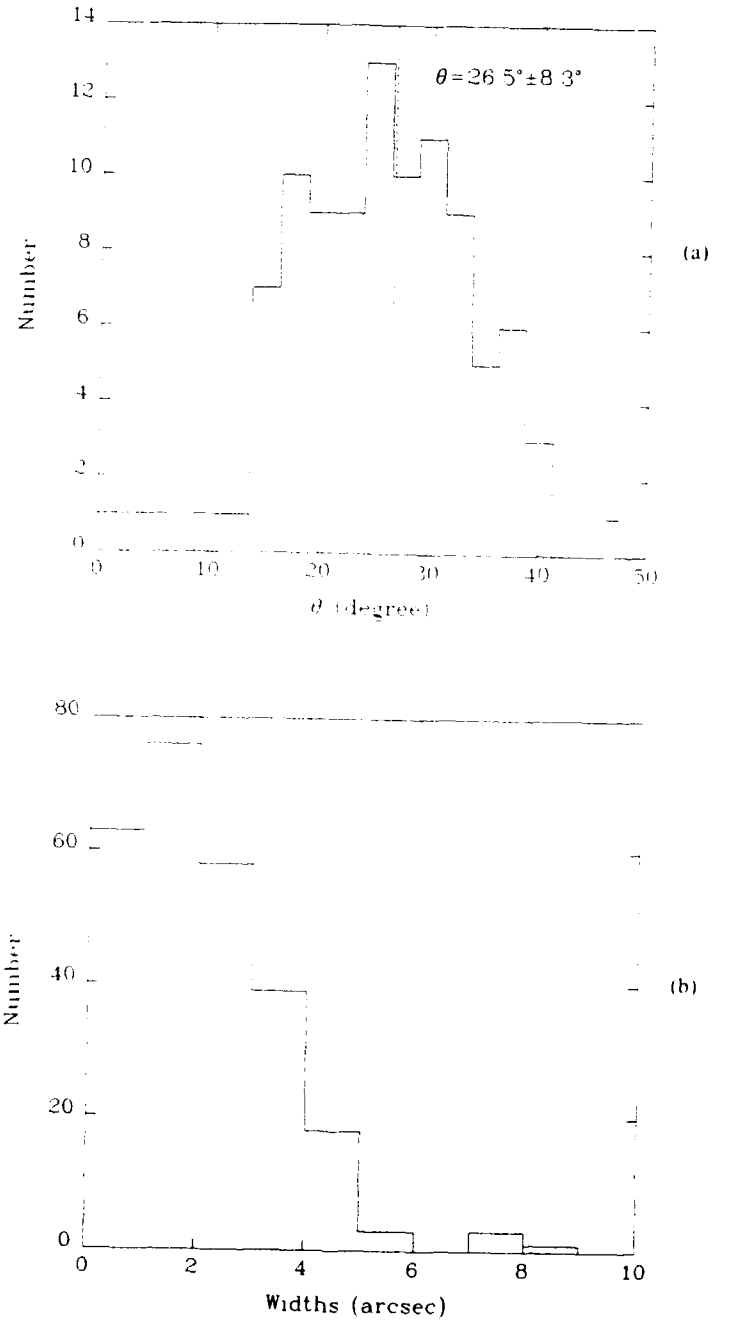

Fig. 2. (a) Distribution of the angles of the filament fibrils with the long axis of the filament and (b) fibril widths of the May 4 filament.

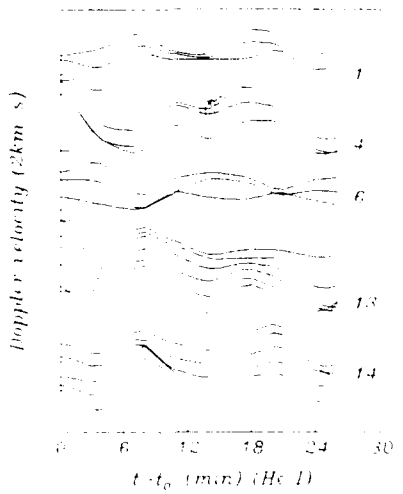

Fig. 3. Curves showing oscillations in the Doppler velocity of He I λ10830 Å for the May 4 filament (t_0 = 13:41:00 UT). The numbers refer to the fibrils shown in Figure 1. The differences in the signals from various fibrils are obvious. Power spectrum analysis yields oscillatory periods ranging from 9 to 14 min.

intensity and velocity images derived for the region of this filament. The corresponding time curves and power spectra are shown in Figure 5. The oscillatory character that can be seen in the graphs shows up as maxima in the power spectra at frequencies between 3 mHz and 1 mHz. These frequency values are equivalent to periods of about 5 min and 16 min.

Data from the photospheric Si I line (Figures 6 and 7) reveals, as expected, a dominant power peak around 3 mHz (5 min). In addition, there are hints of periods around 14 min in the photospheric regions below the filament.

3.2.2. *Intensity*

In contrast to results from earlier studies, a pronounced oscillatory variation shows up in the He I line center at several positions along the large fibril of the 3 May filament. The intensity curves and the average power spectrum are presented in Figures 8(a) and 8(b), showing oscillations with amplitudes of about 2% of the local continuum intensity. The curves have been corrected for variations in atmospheric transparency which also give rise to some intensity fluctuation. These corrections are done with the help of simultaneously recorded, spatially-averaged continuum intensity values of the time series. The two dominant periods in the intensity fluctuations of about 5 and 12 min are virtually the same as in the case of the velocity signal.

A cross-correlation of the velocity and intensity reveals a phase dependence of the two signals (Figure 9(a)). The largest negative shifts occur at maximum intensity. In addition, there is often an increased negative correlation close to $\Delta t \sim -5$ min, i.e.,

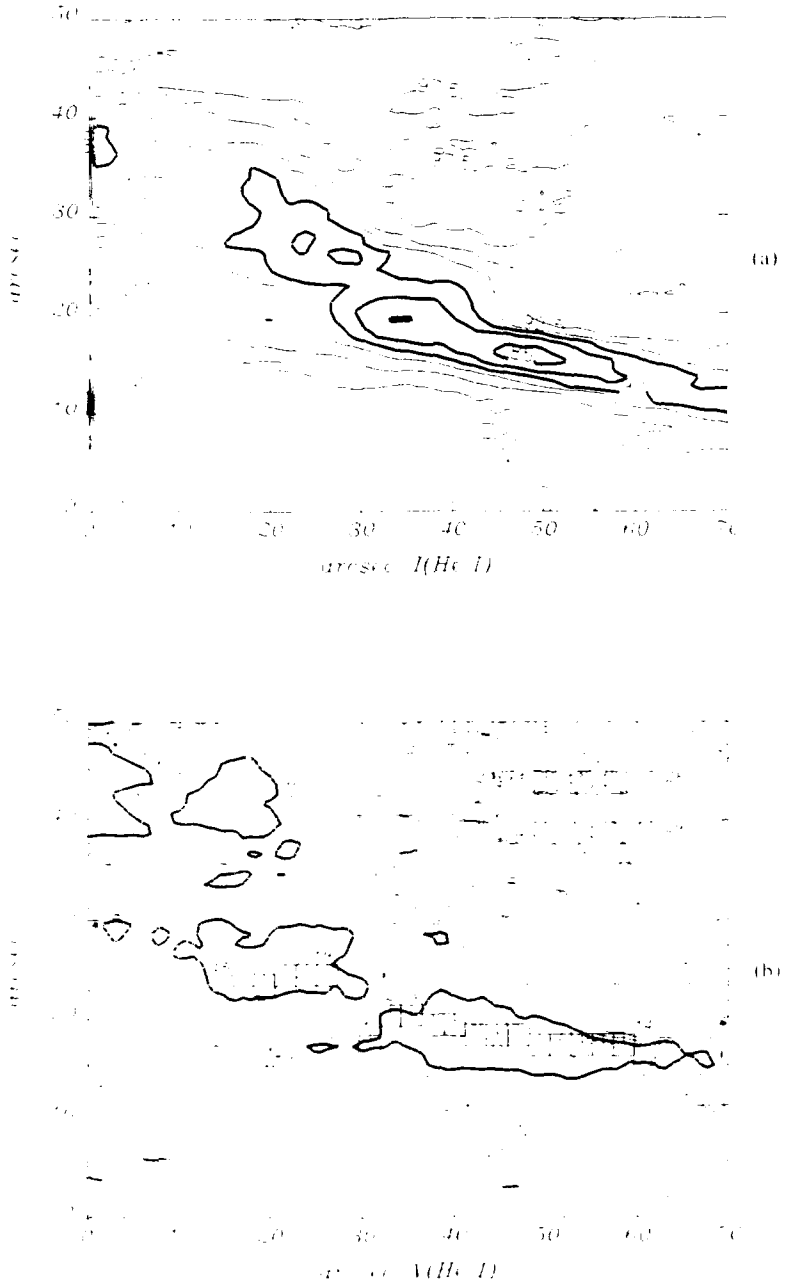

FIG. 4. (a) Contour map of the central intensity of He I 10830 Å line of a filament observed on May 3, 1981, 14:44:20 UT. (b) The corresponding velocity field of the He I line. The small 'squares' give the sampling positions and areas.

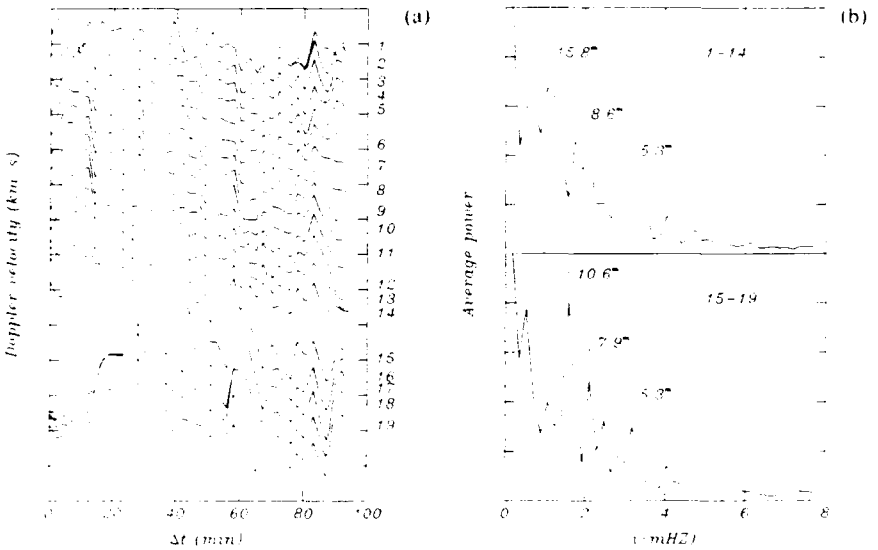

Fig. 5 Oscillations of He I λ10830 Å velocity field inside the filament: (a) Velocity curves. The numbers given to the right correspond to the positions shown in Figure 4(b); (b) the average power spectra. Periods around 15.8, 8.6, and 5.3 min are outstanding for the first fibril (1–14), and around 10.6 min for the second fibril.

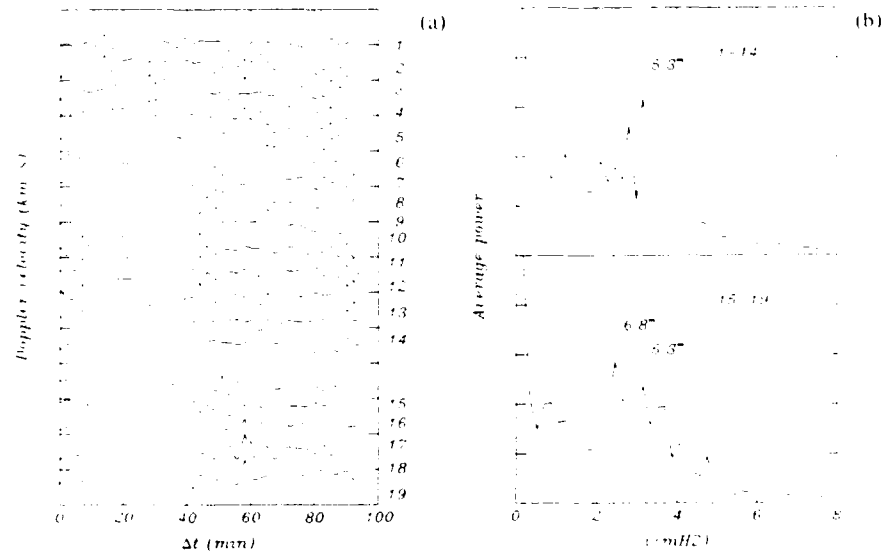

Fig. 6 Oscillations in Si II λ10827.109 Å velocity below the filament. (a) Velocity curves, and (b) averaged power spectra. The 5-min oscillations are observable in the photospheric layer.

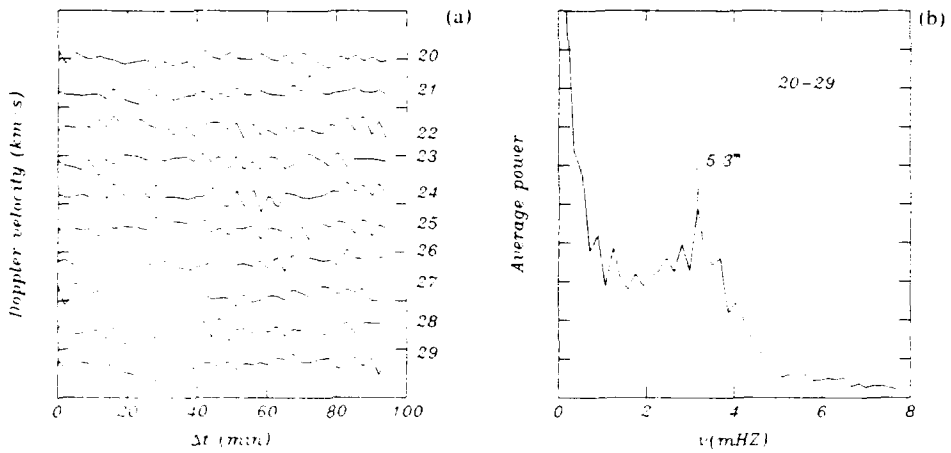

Fig. 7. Oscillations in SiI λ10827.109 Å velocity in regions outside the filament: (a) Velocity curves, and (b) averaged power spectra. The 5-min period is also detectable in this area.

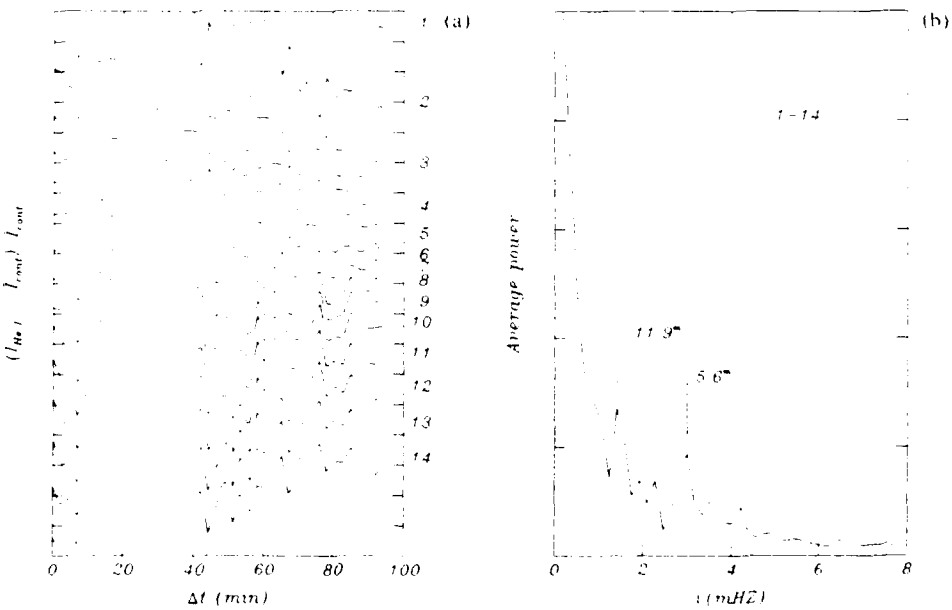

Fig. 8. Intensity variations in HeI λ10830 Å line. The positions are the same as for the velocity curves shown in the previous figures. (a) Intensity variations corrected for seeing (see text), and (b) averaged power spectrum.

Fig. 9. Cross-correlation of the He I velocity and intensity variations. (a) Examples of the most commonly observed phase dependence. (b) A case which is rarely observed.

approximately one full period of the oscillation. This suggests that the intensity variations often show up one period after the start of the velocity oscillation. In one case (Figure 9(b)) the opposite situation, namely that the intensity is preceeding the velocity oscillation, is occasionally seen.

Assuming that the intensity signal is produced by variations in seeing, as suggested by Ghenojian, Klepikov, and Stepanov (1990), one would expect similar type signals in the Si I and the water vapour lines. The Si I central intensity also varies, but the variation is different from the He I λ10830 Å line. One may, therefore, conclude that the observed intensity variations can not be ascribed to seeing.

3.3. Lifetime of Fine-Scale Structures

One notices that the observed periods of oscillations are comparable to the lifetime of fine-scale structures (thread and knots) of quiescent prominences (Engvold, 1976). Unfortunately, the contrast of the present He I images of disk filament is too low to resolve well the individual threads for a direct determination of their lifetimes. By taking the cross-correlation of the intensity images of the filament one may, however, derive an average time property for the structure.

Using the definition of lifetime given by Golub (1976), we may introduce the values $C(t - t_0)$, which are the cross-correlation coefficients as functions of time. In Figure 10 we have plotted the time cross-correlation for the filament area of the 3 May event. The curve appears to be the result of two different lifetimes τ_1 and τ_2 which can be represented by the formula:

$$C(t - t_0) = c_1 e^{-(t - t_0)/\tau_1} + c_2 e^{-(t - t_0)/\tau_2}, \tag{1}$$

where t_0 is the time of observation of the reference frame and τ_1 and τ_2 represent the two time-scales. The time scales for small-scale, medium-scale, and large-scale structures of prominences are generally taken to be, respectively, ≤ 10 min, 2–12 hours, and weeks to months (Engvold *et al.*, 1989). In the event that the shorter scale τ_1 is only a few minutes and τ_2 is several hours the relation may be expressed by the two alternative expressions:

$$C(t - t_0) \approx \begin{cases} c_2 + c_1 e^{-(t - t_0)/\tau_1}, & t - t_0 \ll \tau_2, \\ c_2 e^{-(t - t_0)/\tau_2}, & t - t_0 \gg \tau_1. \end{cases} \tag{2}$$

A fit of the curve in Figure 10 to the expressions above yields $\tau_1 \simeq 13$ min, which is in good agreement with values for small-scale structures obtained by others.

The similarity of the periods of velocity oscillations and the time-scale τ_1 may imply a possible phase dependence between velocity and brightness. We also noted an increase of cross-correlation coefficients at about one hour later. This quasi-oscillation in intensity will influence the lifetime of the prominence structures determined by cross-correlation techniques.

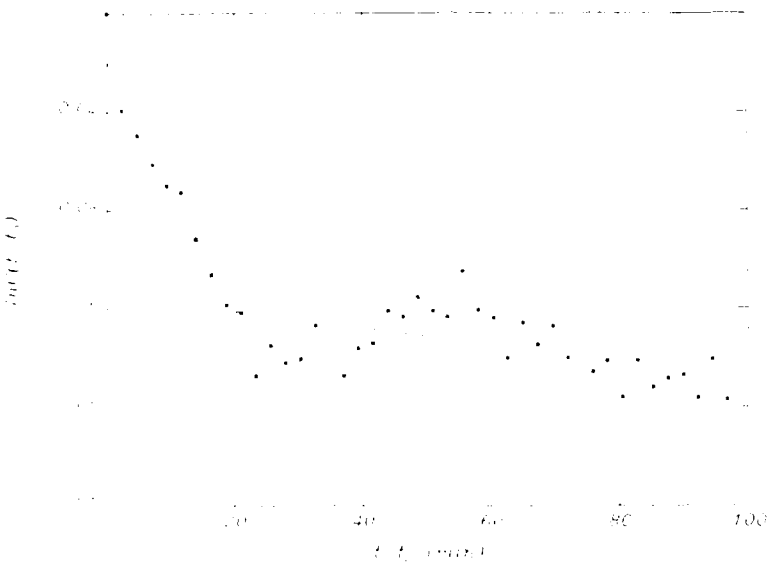

Fig. 10. Cross-correlation of He I intensity in the time series from the May 3 filament. Two different time-scales are apparent from the plot. Similar curves are found for other filaments of our data.

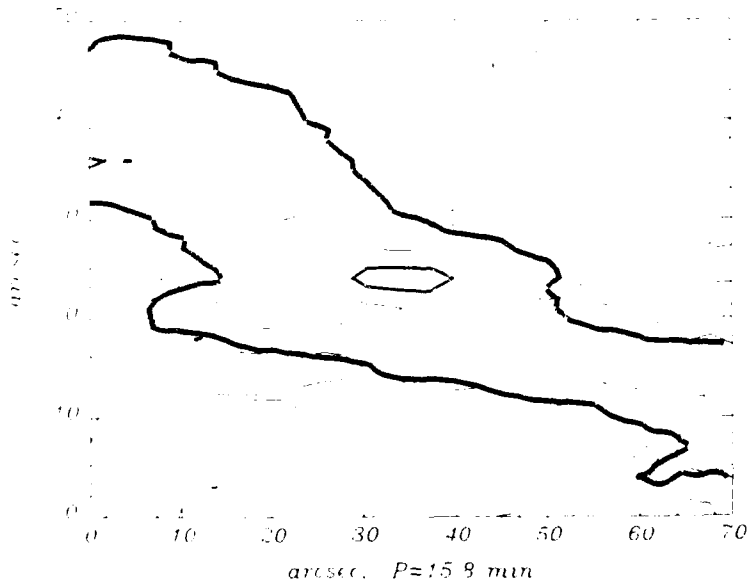

Fig. 11a.

Fig. 11. The distribution of oscillatory periods in He I λ10830 Å velocity for the power maxima at, respectively, P = 15.8, 10.6, 8.6, and 5.3 min (see Figure 5(b)). The He I λ10830 Å intensity contours corresponding to 30%, 50%, and 70% of the maximum power are shown by, respectively, solid, dotted, and bold lines. The two heavy lines mark the filament channel.

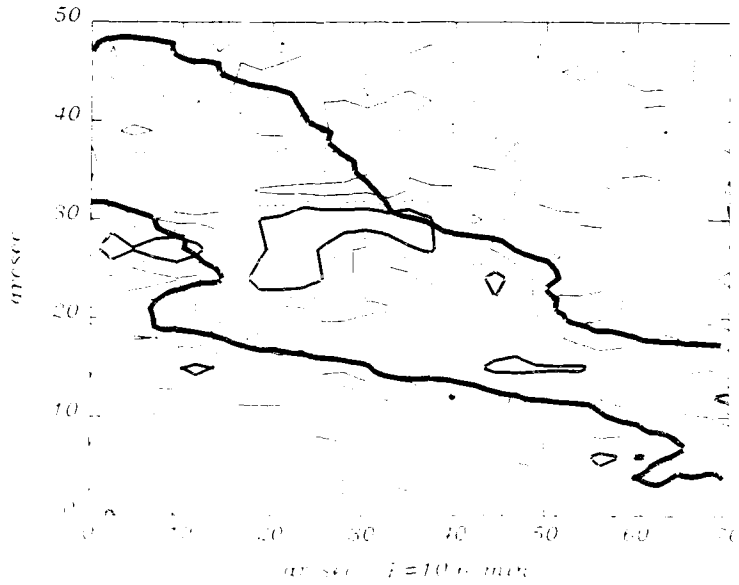

Fig. 11b.

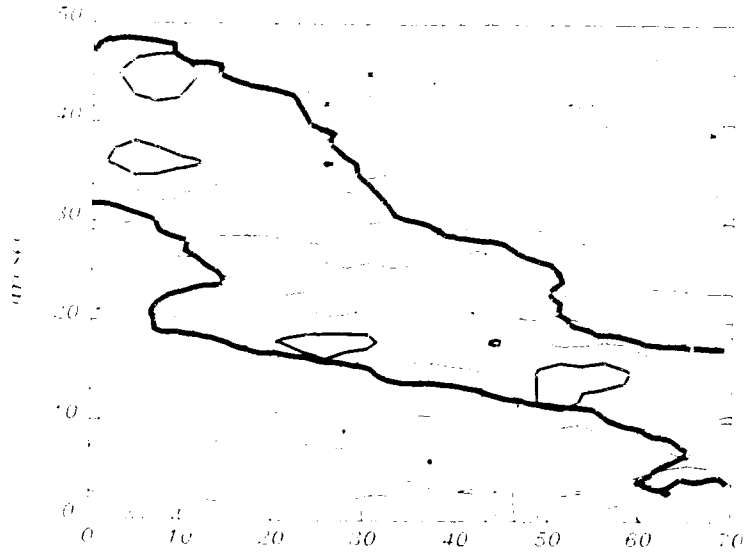

Fig. 11c.

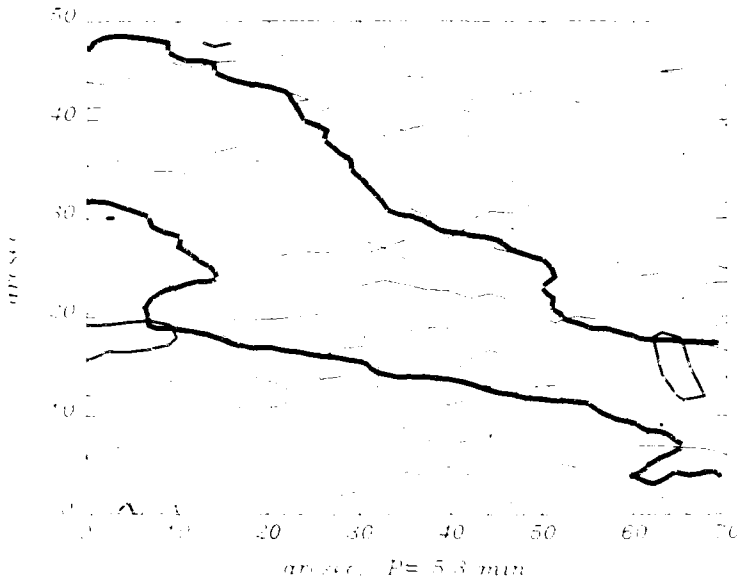

Fig. 11d.

3.4. Spatial Distribution of Oscillatory Periods

Each point in the field has its own time property which can be studied from power spectra derived for every point (e.g. area 2.5 × 3.0 arc sec^2). For a given frequency of the oscillations one derives the distribution of power as function of position within the observed area. Figure 11 shows the distribution of oscillating regions derived from the He I velocity field. The selected frequencies correspond to peaks in the power spectra.

The filament channel is clearly seen in the maps showing the power distribution at frequencies of power maxima in the spectra. The filaments are, on the other hand, not noticeable in maps based on frequencies of power minima of the spectra.

The similarity of the time variations at the positions, respectively, 1–14 and 15–19 in Figure 5a, suggests that these are two separate magnetic loop structures. The oscillatory power is notably suppressed in the region between the two fibrils.

Unlike the results from the He I λ10830 Å, the Si I line shows mainly the 5-min period. Some correlation is seen between various power peaks of the photospheric Si I line and the outline of the filament. This could possibly be where the 'foot-points' of filaments connect to the photosphere. At all other frequencies the oscillatory periods are irregularly distributed.

4. Conclusion

4.1. Structures

The velocity images derived from the He I λ10830 A line provide better contrast than the corresponding intensity images, and resolve clearly the fine-scale fibril structures. These structures represent mass motion in magnetic tubes of force. The tendency of the fibrils to be inclined with respect to the long axis of the large filament would agree with the flux tube interpretation. A number of observations have shown that the angle between the field vector and the prominence long axis is typically about 25° (Leroy, Bommier, and Sahal-Brechot, 1983, 1984; Kim *et al.*, 1988) in good agreement with the current angles of inclination given in Figure 2.

4.2. Oscillations

The oscillatory character of large quiescent disk filaments is apparent in the observations of the He I λ10830 A line. The measured periods of about 10 min are very similar to the values obtained from prominences observed at the Sun's limb. The amplitudes of velocity fluctuations around 0.5 km s^{-1} are generally less than the values derived from observations at the limb (Tsubaki, Ohnishi, and Suematsu, 1987). It is likely that the spatial resolution of our data ($\sim$ 1 arc sec) would tend to smear the signal and thereby reduce the velocity amplitudes.

Since the chromospheric He I λ10830 A line is very weak there will be no chromospheric contribution to the Doppler shifts in the filament. The measured Doppler velocities are produced in the filaments.

The fact that the characteristic 5-min oscillation period of the photosphere, is clearly present in the two large fibrils seen in Figure 4(b) (see Figure 5(b)), could suggest that the photospheric motions trigger the oscillations in the prominence. The 8-min to 16-min periods, that are observed in the fibrils, are not apparent in the power spectrum of the photospheric Si I line. These longer period oscillations in the filament could in turn be generated by agitation at its footpoint where the 5-min period is dominant.

The observed oscillatory changes in He I central intensity cannot be ascribed to seeing or other atmospheric effects, and they are, therefore, deemed to be of solar origin. It is of interest to compare the radiative energies associated with these oscillations with estimates of potentially available mechanical energies in the fibril structures. Using a continuum intensity $I_c^{10830} \sim 1.0 \times 10^6$ erg cm^{-2} s^{-1} sr^{-1} A^{-1}) (Labs and Neckel, 1970, 1973), the intensity amplitude of $\sim 2\%$ in the central intensity of the He I line ($\Delta\lambda \simeq 0.5$ A) associated with these fluctuations corresponds to a radiative flux at λ10830 A; $F_{\text{rad}}^{10830} \sim 10^5$ erg cm^{-2} s^{-1}. Possible variations in line widths, which are normally less than about 20% (see Tsubaki and Takeuchi, 1988), could impose only minor modifications of this amplitude value.

One cannot readily convert these fluctuations into a corresponding value for the total radiative flux variation since different lines respond differently to small changes in the atmospheric parameters. We may, however, attempt to make an order of magnitude

estimate of the fluctuation in the total flux by considering the brightness of the He I line to other bright emission lines of prominences. Using line fluxes of quiescent prominences observed by Yakovkin and Zeldina (1964), Engvold (1978), Milkey *et al.* (1978), Vial (1982), and others, together with values of the line emission predicted from theoretical models of prominences (Heasley and Milkey, 1976), one finds that the total emission from a prominence is easily ≥ 20 times the flux from the He I λ10830 line alone. From this we estimate the observed fluctuations in the emission of a quiescent prominence to be $F_{\text{rad}} = 2 \times 10^6$ erg cm^{-2} s^{-1}.

An estimate of a possible MHD wave energy flux in the fibril structures may be derived from the expression

$$F_w \simeq \tfrac{1}{2}\rho(\Delta V)^2 V_A , \tag{3}$$

where ρ is the gas density, ΔV the amplitude velocity of the oscillations, and V_A an assumed Alfven velocity. Using the values $\rho \simeq 10^{-13}$ g cm^{-3}, $\Delta V \simeq 2$ km s^{-1}, and $V_A \simeq 70$ km s^{-1} and get $F_w \sim 1.4 \times 10^4$ erg cm^{-2} s^{-1}.

One may assume that a fraction χ of this flux is converted to radiative energy per unit length, and that the thickness of the fibril structure in the line-of-sight is L. The resulting radiative flux should then be $F \sim \chi F_w L$. Looking nearly perpendicular to the fibril structure of thickness $L = 10^2$–10^3 km (Engvold *et al.*, 1989), one obtains values for F in the range $1.4 \times 10^{11}\chi$ to $1.4 \times 10^{12}\chi$ (erg cm^{-2} s^{-1}), which compared with the estimated values of F_{rad} above would yield $\chi \leq 10^{-5}$. Hence, the radiative energy associated with the oscillations appears negligibly small in comparison with estimates of wave energy in the structures.

On the other hand, weak dissipation coupled to density fluctuations driven by Alfvén waves (Hollweg, 1971) in the filament fibrils could account for the observed intensity variations, but the waves would need to undergo negligible damping for this reason.

The time behaviour of the velocity is strikingly similar for different points along a given filament fibril (points 1–14, and 15–19 in Figure 5(a)) showing that the entire fibril structure takes part in the motion. It has been proposed that oscillations with periods 3–11 min could be Alfvén waves propagating along magnetic loops of solar prominences (Solov'ev, 1985). Jensen (1983, 1989) has shown that dissipation of Alfvénic wave energy in prominences may provide support in the field of gravity. The search for phase velocities in the oscillating filament fibrils, and the possible Alfvénic character of these oscillations is discussed in a subsequent paper (Yi Zhang, Engvold, and Jensen, 1991).

4.3. Lifetimes

It has been noticed that the observed periods of oscillations are comparable to the lifetime of the fine-scale structures (threads and knots) of quiescent prominences (Engvold, 1976). Suematsu *et al.* (1990) noticed quasi-oscillatory intensity variations of periods ~ 10 min in the Ca II K line from a quiescent prominence, which agrees well with the oscillatory periods measured in the present data. Cross-correlation of the filament image gives an e-folding time of ~ 13 min, in good agreement with the above.

The fact that the fibril structures are moving, partly due to oscillatory motions, and partly because motions in the photosphere will displace thin magnetic flux ropes forming the fibrils, will lead to a continuous restructuring of the small-scale fibrils. Assuming photospheric flow velocities of ≤ 0.5 km s^{-1}, the anchor points of flux ropes could move a distance comparable to the observed scale of the fibrils (≤ 300 km) in ~ 10 min. Cross-correlation analysis may then lead to lifetimes of similar values.

In conclusion, the measured lifetimes of the small-scale structures in prominences (filaments) very likely reflect combination of (i) intensity modulations and (ii) physical reshuffling of small-scale fibril structure.

Acknowledgement

The authors thank Prof. Eberhart Jensen for invaluable comments and suggestions in the course of this work.

References

Balthasar, H., Knölker, M., Stellmacher, G., and Wiehr, E.: 1986, *Astron. Astrophys.* **163**, 343.
Bahskirtsev, V. S. and Mashnich, G. P.: 1984, *Solar Phys.* **91**, 93.
Breckinridge, J. B. and Hall, D. N. B.: 1973, *Solar Phys.* **28**, 15.
Demoulin, P., Raadu, M. A., Malherbe, J. M., and Schmieder, B.: 1987, *Astron. Astrophys.* **183**, 142.
Dunn, R. B.: 1960, Ph.D. Thesis, Harvard University.
Dunn, R. B.: 1969, *Sky Telesc.* **38**, 368.
Engvold, O.: 1976, *Solar Phys.* **49**, 283.
Engvold, O.: 1978, *Solar Phys.* **56**, 87.
Engvold, O., Malville, J. M., and Livingston, W.: 1978, *Solar Phys.* **60**, 57.
Engvold, O., Hirayama, T., Leroy, J.-L., Priest, E. R., and Tandberg-Hanssen, E.: 1989, in V. Ruždjak and E. Tandberg-Hanssen (eds.), *Proc. IAU Colloq.* **119**.
Ghenoujan, L. V., Klepikov, V. Yu., and Stepanov, A. I.: 1990, 'Academy of Sciences of the USSR, IZMIRAN, Reprint No. 4.
Giovanelli, R. G., Hall, D. N. B., and Harvey, J. W.: 1972, *Solar Phys.* **22**, 53.
Golub, L.: 1976, *Solar Phys.* **46**, 115.
Heasley, J. N. and Milkey, R. W.: 1976, *Astrophys. J.* **210**, 827.
Hollweg, J. V.: 1971, *J. Geophys. Res.* **76**, 5155.
Jensen, E.: 1983, *Solar Phys.* **89**, 275.
Jensen, E.: 1989, in 'Dynamics of Prominences', V. Ruždjak and E. Tandberg-Hanssen (eds.), *Proc. IAU Colloq.* **119**.
Kim, I. S.: 1990, 'Prominence Magnetic Field Observations', Preprint 11 from GAIS, Sternberg State Astronomical Institute, Moscow State University.
Labs, D. and Neckel, H.: 1970, *Solar Phys.* **15**, 79.
Labs, D. and Neckel, H.: 1973, *Proceedings of Symposium on Solar Radiation*, Smithsonian Institution, Washington, D.C., 269.
Leroy, J. L., Bommier, V., and Sahal-Brechot, S.: 1983, *Solar Phys.* **83**, 135.
Leroy, J. L., Bommier, V., and Sahal-Brechot, S.: 1983, *Astron. Astrophys.* **131**, 33.
Malherbe, J. M., Schmieder, B., and Mein, P.: 1981, *Astron. Astrophys.* **55**, 103.
Malherbe, J. M., Schmieder, B., Mein, P., and Tandberg-Hanssen, E.: 1987, *Astron. Astrophys.* **172**, 316.
Malville, J. M. and Schindler, M.: 1981, *Solar Phys.* **70**, 115.
Milkey, R. W., Heasley, J. N., Schmahl, E. J., and Engvold, O.: 1978, in E. Jensen, P. Maltby, and F. Orrall (eds.), 'Physics of Solar Prominences' *IAU Colloq.* **44**, 53.
Simon, G., Schmieder, B., Demoulin, P., and Poland, A. I.: 1986, *Astron. Astrophys.* **166**, 319.
Solov'ev, A. A.: 1985, *Soln. Dannye* No. 9, 65.

Suematsu, Y., Yoshinaga, R., Terao, N., and Tsubaki, T.: 1990, *Publ. Astron. Soc. Japan* **42**, 187.
Tandberg-Hanssen, E. and Anzer, U.: 1970, *Solar Phys.* **15**, 158.
Tsubaki, T. and Takeuchi, A.: 1986, *Solar Phys.* **104**, 313.
Tsubaki, T., Ohnishi, Y., and Suematsu, Y.: 1987, *Publ. Astron. Soc. Japan* **39**, 179.
Tsubaki, T., Toyoda, M., Suematsu, Y., and Gamboa, G. A. R.: 1988, *Publ. Astron. Soc. Japan* **40**, 121.
Uchida, Y.: 1980, in F. Moriyama and J. C. Hénoux (eds.), *Proceedings of 'The Japan-France Seminar on Solar Physics'*, p. 169.
Vial, J. C.: 1982, *Astrophys. J.* **254**, 780.
Wiehr, E., Stellmacher, G., and Balthasar, H.: 1984, *Solar Phys.* **94**, 285.
Yakovkin, N. A. and Zel-dina, M. Yu.: 1964, *Soviet Astron.-AJ* **7**, 643.
Yi Zhang, Engvold, O., and Jensen, E.: 1991, in preparation.